RadioGraphics

Masses and Malformations of the Third Ventricle: Normal Anatomic Relationships and Differential Diagnoses[1]

Christine M. Glastonbury, MBBS • Anne G. Osborn, MD • Karen L. Salzman, MD

ONLINE-ONLY CME

See www.rsna.org/education/rg_cme.html

LEARNING OBJECTIVES

After completing this journal-based CME activity, participants will be able to:

- Describe the normal anatomic landmarks of the third ventricle and key anatomic relationships that are important for imaging evaluation of intracranial lesions.
- Discuss creation of differential diagnoses for third ventricle masses on the basis of their location with respect to the ventricle contours.
- Identify intraventricular masses of the third ventricle.

TEACHING POINTS

See last page

The third ventricle lies in the center of the brain. It is surrounded by critical nuclear structures (the hypothalamus and thalami) and important glandular structures (the pituitary and pineal glands). Although a wide array of pathologic processes may involve the third ventricle, most are extrinsic masses. By understanding the anatomic boundaries of the third ventricle and its relationship to adjacent structures, it is possible to create short lists of differential diagnoses. Third ventricle masses can be classified as arising in or immediately adjacent to one of five locations: anterior, posterior, inferior, foramen of Monro, and intraventricular. Anterior masses involve the optic and infundibular recesses, posterior masses affect or arise in the posterior commissure and pineal gland, and inferior masses involve or affect the ventricle floor. Masses may also arise at or adjacent to the foramen of Monro or entirely within the third ventricle. Of the intraventricular masses, chordoid glioma—a rare low-grade primary neoplasm—is unique to the third ventricle. Congenital malformations of the third ventricle are uncommon and are most often noted during childhood. Most commonly, these anomalies represent malformations of the neurohypophysis, which may manifest as hormonal abnormalities, or stenosis of the aqueduct of Sylvius, which manifests as dilatation of the third and lateral ventricles (hydrocephalus).

Abbreviations: CPP = choroid plexus papilloma, CSF = cerebrospinal fluid, FLAIR = fluid-attenuated inversion-recovery, SGCT = subependymal giant cell tumor, TSC = tuberous sclerosis complex, WHO = World Health Organization

RadioGraphics 2011; 31:1889–1905 • **Published online** 10.1148/rg.317115083 • **Content Codes:** NR OI

[1]From the Department of Radiology and Biomedical Imaging, University of California, San Francisco, 505 Parnassus Ave, Box 0628, Room L-358, San Francisco, CA 94143-0628 (C.M.G.); and Department of Radiology, University of Utah Health Sciences Center, Salt Lake City, Utah (A.G.O., K.L.S.). Recipient of a Cum Laude award for an education exhibit at the 2010 RSNA Annual Meeting. Received April 13, 2011; revision requested June 22 and received July 12; accepted July 19. For this journal-based CME activity, the authors C.M.G., A.G.O., and K.L.S. have disclosed various financial relationships (see p 1904); the editor and reviewers have no relevant relationships to disclose. **Address correspondence to** C.M.G. (e-mail: *christine.glastonbury@ucsf.edu*).

Introduction

Lesions of the third ventricle can have a variety of clinical manifestations. Masses related to the anterior recesses or floor of the third ventricle may manifest as dysfunction of the hypothalamic–pituitary gland axis. Masses of the posterior wall of the third ventricle, foramen of Monro masses, and intraventricular masses often manifest as hydrocephalus and headaches. Some congenital cysts or acquired abnormalities, such as cavum veli interpositi cyst and ectatic basilar artery, respectively, may be incidental imaging findings but distort the normal anatomy of the third ventricle or mimic more serious disease.

In this article, we present a practical review of congenital anomalies and acquired pathologic processes of the third ventricle, with a focus on those lesions that are unique to the third ventricle. Our primary focus is to help radiologists differentiate the vast array of potential pathologic processes and to clarify key findings that are important for the surgical approach to third ventricle lesions. To this end, it is important to first have a clear understanding of the normal anatomic landmarks of the third ventricle and the key anatomic relationships. Although computed tomography (CT) may be the initial study for symptoms related to a third ventricle mass, magnetic resonance (MR) imaging is superior for delineating such a mass, demonstrating its site of origin, and permitting planning of a surgical approach for biopsy or resection.

CT and MR Imaging Anatomy of the Third Ventricle

The third ventricle lies in the midline of the diencephalon. In the axial and coronal planes, it has a slitlike contour; in the sagittal plane, it has a complex fishlike shape created by two anterior and two posterior recesses and a curving roof and floor (Fig 1). Most of the lateral walls of the ventricle are formed by the medial aspects of the two thalami, which communicate in the midline along a band of gray matter known as the massa intermedia. The inferior aspect of the third ventricle lateral walls is formed by the hypothalamus anteriorly and the subthalamus posteriorly (2,3).

The key components of the anterior contour and floor of the third ventricle are best identified in the sagittal plane (Fig 1). The superior limit is the anterior commissure, a key surgical landmark, while the lamina terminalis forms the anterior wall descending to the optic chiasm. The anterior "fish mouth" shape of the third ventricle is created by two recesses, the optic recess superiorly and the infundibular recess inferiorly. The infundibular recess or pars cava infundibuli is formed by the funnel-shaped proximal hypothalamic infundibulum (pituitary stalk). Around the base of the infundibulum is the median eminence, a raised portion of hypothalamic gray matter. The median eminence and the tuber cinereum, which is also part of the hypothalamus, form most of the floor of the third ventricle. These portions of the hypothalamus lack a blood-brain barrier and typically enhance with gadolinium on MR images. The mammillary bodies and midbrain posterior to the tuber cinereum form the posterior aspect of the floor of the third ventricle and do not normally enhance on MR images.

The most readily identified anatomic landmark of the posterior contour of the third ventricle is the pineal gland, but there are also two recesses and two commissures to note. The pineal recess of the third ventricle is in the deep aspect of the pineal gland. The posterior commissure is in the inferior wall of this pineal recess, while the habenular commissure fibers form in the superior wall of the pineal recess. The suprapineal recess forms above the habenular commissure, lying below the splenium of the corpus callosum.

The roof of the third ventricle is best described as having five layers: the body of the fornix, the superior layer of tela choroidea, the vascular layer, the inferior layer of tela choroidea, and the choroid plexus of the third ventricle, which is inseparable from the tela choroidea (4,5). The bilaminar tela choroidea stretches beneath the body of the fornix, is closed anteriorly at the foramen of Monro, and contains the vascular layer of the third ventricle roof. The vascular layer is synonymous with the velum interpositum and contains the internal cerebral veins and the medial posterior choroidal arteries, bathed in cerebrospinal fluid (CSF). When the posterior aspect of the vascular layer is open, it communicates with the quadrigeminal cistern and is known as the cavum veli interpositi (6).

The interventricular foramen of Monro allows the two lateral ventricles to communicate with each other and with the third ventricle (Fig 2). The foramen is located posterior to the anterior

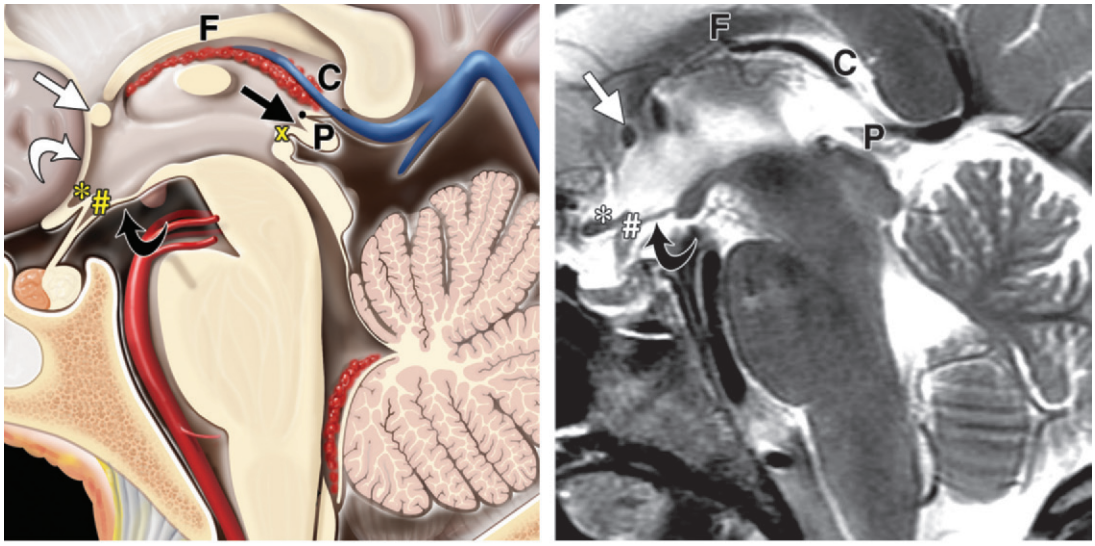

Figure 1. Normal anatomic landmarks in the sagittal plane. Sagittal diagram **(a)** and T2-weighted MR image **(b)** show some of the key landmarks of the third ventricle: the anterior commissure (straight white arrow), cavum veli interpositi *(C)*, fornix *(F)*, habenular commissure (black dot in **a**), infundibular recess (#), lamina terminalis (curved white arrow in **a**), optic recess (∗), pineal gland *(P)*, pineal recess (straight black arrow in **a**), posterior commissure (*x* in **a**), and tuber cinereum (curved black arrow). (Diagram reprinted, with permission, from reference 1.)

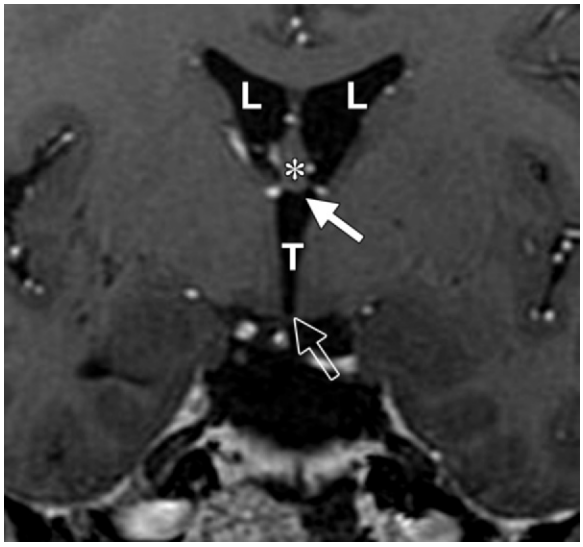

Figure 2. Normal anatomic landmarks: foramen of Monro. Coronal gadolinium-enhanced T1-weighted MR image shows the Y-shaped contour of the foramen of Monro (solid arrow), which allows the two lateral ventricles *(L)* and the third ventricle *(T)* to communicate. ∗ = fornix, open arrow = floor of the third ventricle.

columns of the fornix. Some anatomists describe it as one Y-shaped foramen; others describe it as right and left foramina that communicate with the third ventricle (2,3,7). The egress of CSF from the third ventricle occurs through the cerebral aqueduct of Sylvius, the opening of which is at the posterior aspect of the third ventricle, below the posterior commissure.

Congenital Malformations and Lesions of the Third Ventricle

Congenital malformations and lesions of the third ventricle cover a spectrum of anomalies. Atresia of the third ventricle is rare, results from thalamic fusion, and is associated with other malformations of midline intracranial structures and lateral ventricular dilatation (8). The most common cause of an abnormal contour of the third ventricle is a dilated third ventricle with congenital hydrocephalus. An abnormal contour of the ventricle roof is seen with callosal dysgenesis; an abnormal contour of the anterior aspect of the ventricle is seen with malformations of the neurohypophysis. Congenital cysts may result in an abnormal ventricular contour or may manifest as intraventricular masses.

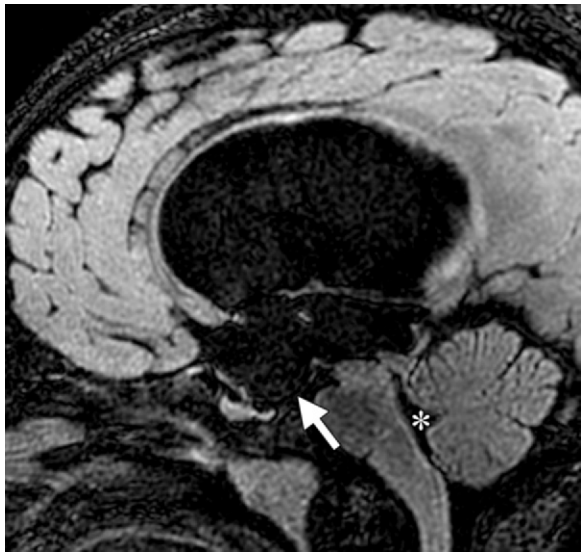

Figure 3. Proximal aqueductal stenosis with marked hydrocephalus in a 17-year-old boy with worsening imbalance and gait instability. Sagittal fluid-attenuated inversion-recovery (FLAIR) MR image shows marked dilatation of the lateral and third ventricles with normal size of the fourth ventricle (*). Note the downward bowing of the third ventricle floor (arrow) with expanded infundibular and optic recesses.

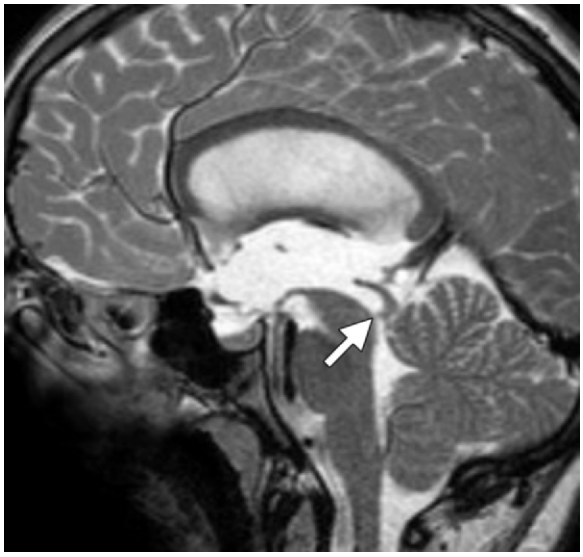

Figure 4. Distal aqueductal stenosis in a 14-year-old boy with seizures and developmental delay. Sagittal T2-weighted MR image shows dilated lateral and third ventricles, a normal-sized fourth ventricle, and a funnel-shaped appearance of the aqueduct (arrow). The funnel-shaped appearance was due to a distal web.

Figure 5. Persistent embryonic infundibular recess in a 25-year-old man who was evaluated with MR imaging for hypogonadotropic hypogonadism. Sagittal T1-weighted MR image shows that the lateral, third, and fourth ventricles are not dilated but the sella is enlarged. The pituitary gland is smaller than expected for the patient's age. The tuber cinereum is depressed (arrow) and the infundibular walls are elongated, creating an expanded infundibular recess (*) that remains in continuity with the third ventricle.

Aqueductal Stenosis

At CT or MR imaging, aqueductal stenosis manifests as dilatation of the third and lateral ventricles that is out of proportion to the fourth ventricle and cerebral sulci. Stenosis most often occurs in the proximal aqueduct and may be congenital or acquired as a postinflammatory aqueductal gliosis. Aqueductal stenosis and hydrocephalus may manifest at any time from fetal age to adulthood, with the age of presentation depending on the severity of the stenosis and hydrocephalus. Up to 10% of adult hydrocephalus cases are due to aqueductal stenosis (9–11).

Teaching Point

As the third ventricle dilates, the anterior recesses become rounded and extend into the suprasellar cistern and the floor of the third ventricle is displaced inferiorly into the prepontine cistern (Fig 3). Distal aqueductal stenosis is less common and may be due to a small web or membrane of tissue that obstructs flow into the fourth ventricle. It results in a funnel contour of the aqueduct in addition to third ventricle dilatation (Fig 4). Distal stenosis may also be due to

a.

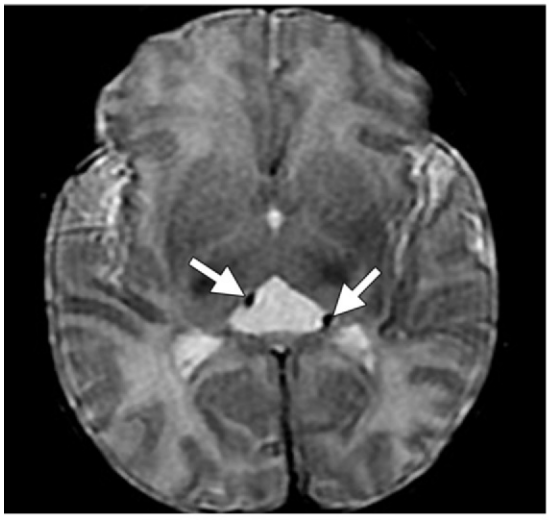

b.

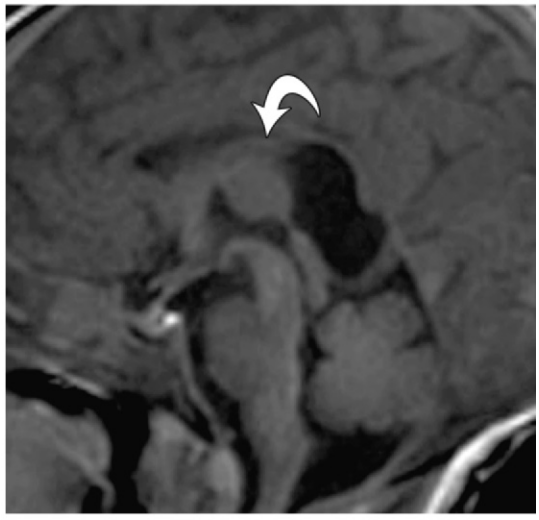

c.

Figure 6. Cavum veli interpositi cyst. Coronal fetal MR image at 35 weeks 2 days gestation **(a)**, axial T2-weighted MR image at 1 day of age **(b)**, and sagittal T1-weighted MR image at 1 day of age **(c)** show a cyst of the cavum veli interpositi below the fornix (arrow in **c**), displacing the internal cerebral veins inferolaterally (arrows in **a** and **b**). The cyst has a characteristic triangular appearance in the axial plane and distorts the posterior superior aspect of the third ventricle in the sagittal plane.

a congenital aqueductal fork, with the aqueduct branching into dorsal and ventral channels (11).

The key imaging differential diagnosis that should be considered for either proximal or distal aqueductal stenosis, particularly in older children or young adults, is a posterior thalamic or tectal neoplasm. Such a neoplasm is best sought on axial and sagittal T2-weighted MR images as a hyperintense mass.

Persistent Embryonic Infundibular Recess

A persistent embryonic infundibular recess is a rare congenital malformation of the neurohypophysis. It appears as unusual expansion of the anterior aspect of the third ventricle into the sella with loss of the contours of the normal recesses. The sella may be expanded and the pituitary gland is typically thinned, a so-called empty sella (12).

At CT or MR imaging, a persistent embryonic infundibular recess may appear as an intrasellar cyst that communicates with the third ventricle. It is proposed to be due to failure of cellular proliferation, which normally obliterates the distal aspect of the embryonal infundibular recess early in gestation (45-mm stage). Abnormal pituitary function is associated with persistent embryonic infundibular recess and may lead to an MR imaging examination that uncovers this anomaly (Fig 5).

Cavum Veli Interpositi Cyst

A cavum veli interpositi cyst is a cyst of the ventricle roof itself, occurring within the two-layered tela choroidea and distorting the posterior superior contour of the third ventricle (6,13). It is typically an incidental finding but may mimic an obstructed third ventricle. The cyst has a triangular contour on axial CT or MR images. Multiplanar MR imaging best demonstrates superior displacement of the fornix and inferolateral displacement of the internal cerebral veins (Fig 6).

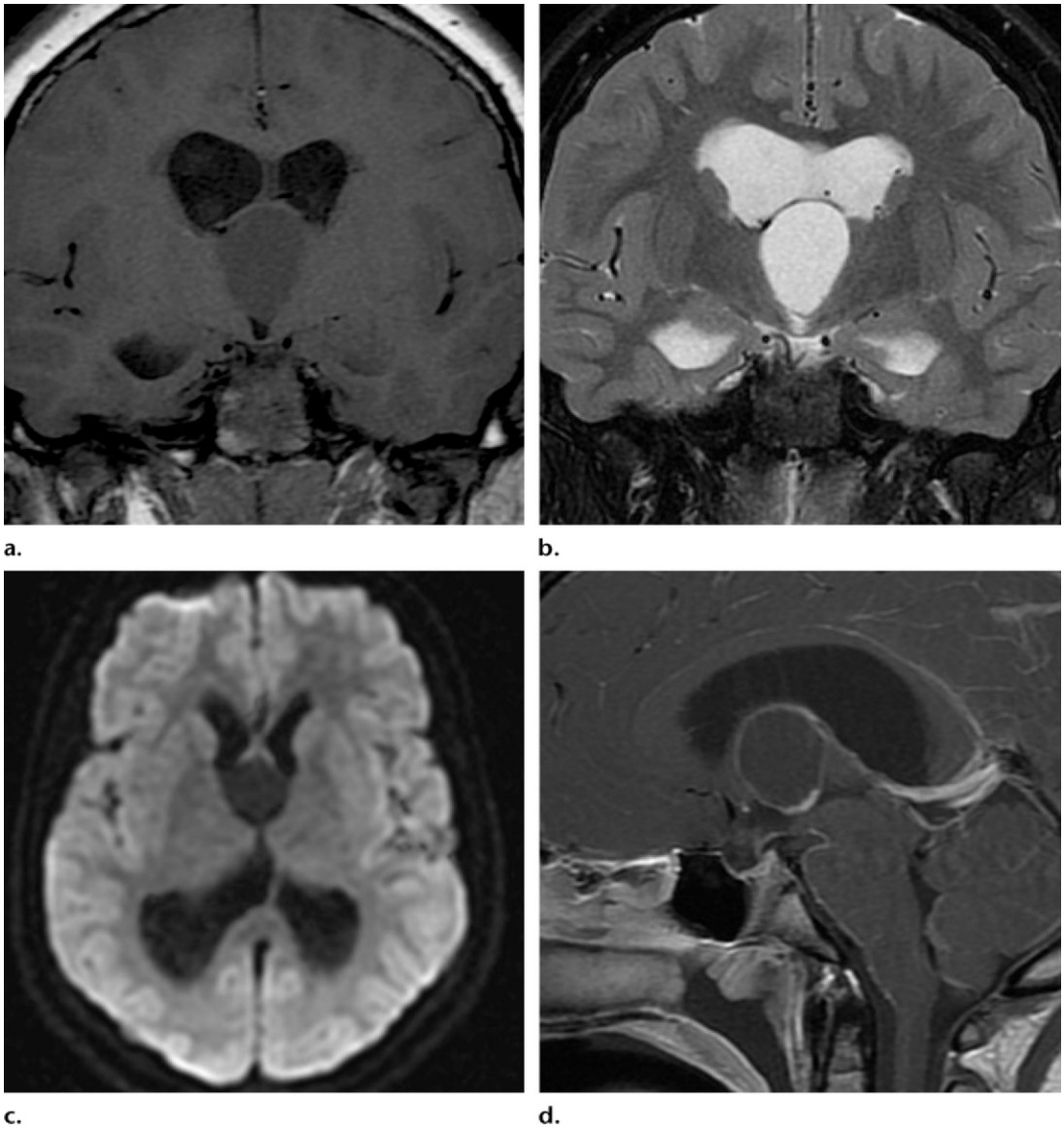

Figure 7. Congenital intraventricular cyst in a 10-year-old girl who was evaluated with MR imaging for precocious puberty. **(a–c)** Coronal T1-weighted **(a)** and T2-weighted **(b)** MR images and axial diffusion-weighted image **(c)** show a cystic lesion located posterior to the anterior commissure, above the third ventricle floor. The lesion elevates the anterior fornices and internal cerebral veins, indicating that it is truly within the third ventricle. **(d)** On a sagittal contrast-enhanced T1-weighted MR image, the lesion has a thin and slightly irregular enhancing rim. After resection, the lesion was determined to be an intraventricular endodermal cyst, which is also known as an enterogenous cyst.

Congenital Intraventricular Cysts

As with most malformations of the third ventricle, congenital intraventricular cysts are rare. They may be of arachnoidal, endodermal, or neuroepithelial origin and most often manifest as hydrocephalus from aqueductal or foramen of Monro obstruction, which may be intermittent. Ependymal cysts are congenital, benign, ependymal-lined cysts that are typically small (several millimeters), asymptomatic, and found in the lateral ventricles. Rarely found in the third ventricle, these have CSF signal intensity with all sequences and do not enhance (14).

MR imaging allows better delineation of intraventricular cysts and has greater sensitivity for detection of an enhancing rim or significant

Table 1
Differential Diagnosis for Third Ventricle Masses by Location

Anterior masses
Sellar-suprasellar masses
Hypothalamic-chiasmatic masses
Posterior masses
Pineal mass
Tectal mass
Inferior thalamic mass
Inferior masses
Hypothalamic hamartoma
Basilar artery ectasia or aneurysm
Arachnoid cyst
Foramen of Monro
Colloid cyst
SGCT with associated TSC
Subependymoma
Intraventricular masses
Primary neoplasm of the choroid plexus*
Metastasis or lymphoma to the choroid plexus or the ventricle proper
Vascular malformation of the choroid plexus
Congenital intraventricular cyst†
Solid neoplasm not of the choroid plexus‡

Note.—SGCT = subependymal giant cell tumor, TSC = tuberous sclerosis complex.
*Papilloma, carcinoma, or lymphoma.
†Arachnoid, ependymal, endodermal, or neuroepithelial cyst.
‡Chordoid glioma, ependymoma, meningioma, or craniopharyngioma.

soft-tissue component (Fig 7), which might indicate a neoplastic lesion such as an intraventricular craniopharyngioma. For a thin-walled cyst, high-resolution heavily T2-weighted MR imaging with a constructive interference in the steady state sequence may allow better delineation of the cyst, which otherwise would appear to be a dilated third ventricle (15).

Acquired Masses of the Third Ventricle

To better understand the variety of pathologic processes that may involve the third ventricle and to allow creation of a useful imaging differential diagnosis, we categorize such processes according to one of five locations with respect to the ventricle (Table 1). Lesions may be found at or involve the anterior aspect of the third ventricle, at the posterior aspect of the ventricle, at or below the ventricle floor, at the foramen of Monro, or within the third ventricle. Entirely intraventricular lesions other than colloid cysts at the foramen of Monro are uncommon, but there is a long imaging differential diagnosis with differentiation often possible on the basis of MR imaging or CT features.

Table 2
Differential Diagnosis for Lesions Distorting or Invading the Anterior Third Ventricle by Age Group

Pediatric patients
Germinoma
Pilocytic astrocytoma
Craniopharyngioma
Langerhans cell histiocytosis
Adult patients
Lymphoma
Pituitary macroadenoma
Craniopharyngioma
Metastases
Granulomatous disease (eg, sarcoidosis)
Sellar meningioma

Anterior Masses

Teaching Point

When masses distort or invade the third ventricle, they most frequently arise in relation to the anterior aspect of the ventricle and can be broadly grouped into sellar-suprasellar masses and hypothalamic-chiasmatic masses. For creation of a useful differential diagnosis, the anterior third ventricle lesions can be further divided into pediatric or adult pathologic processes (Table 2). Of the different pathologic entities that may arise in the sellar or suprasellar region and in the hypothalamus or optic chiasm, some lesions such as germinoma, lymphoma, pituitary macroadenoma, craniopharyngioma, and meningioma may rarely arise entirely within the anterior recesses of the third ventricle (16,17).

Of the pediatric tumors, Langerhans cell histiocytosis most commonly occurs in children under the age of 2 years, whereas the prevalence of germinoma peaks at around 10–12 years. The prevalence of both hypothalamic-chiasmatic pilocytic astrocytoma and craniopharyngioma peaks between the ages of 5 and 15 years. Germinoma arises at the anterior third ventricle less commonly

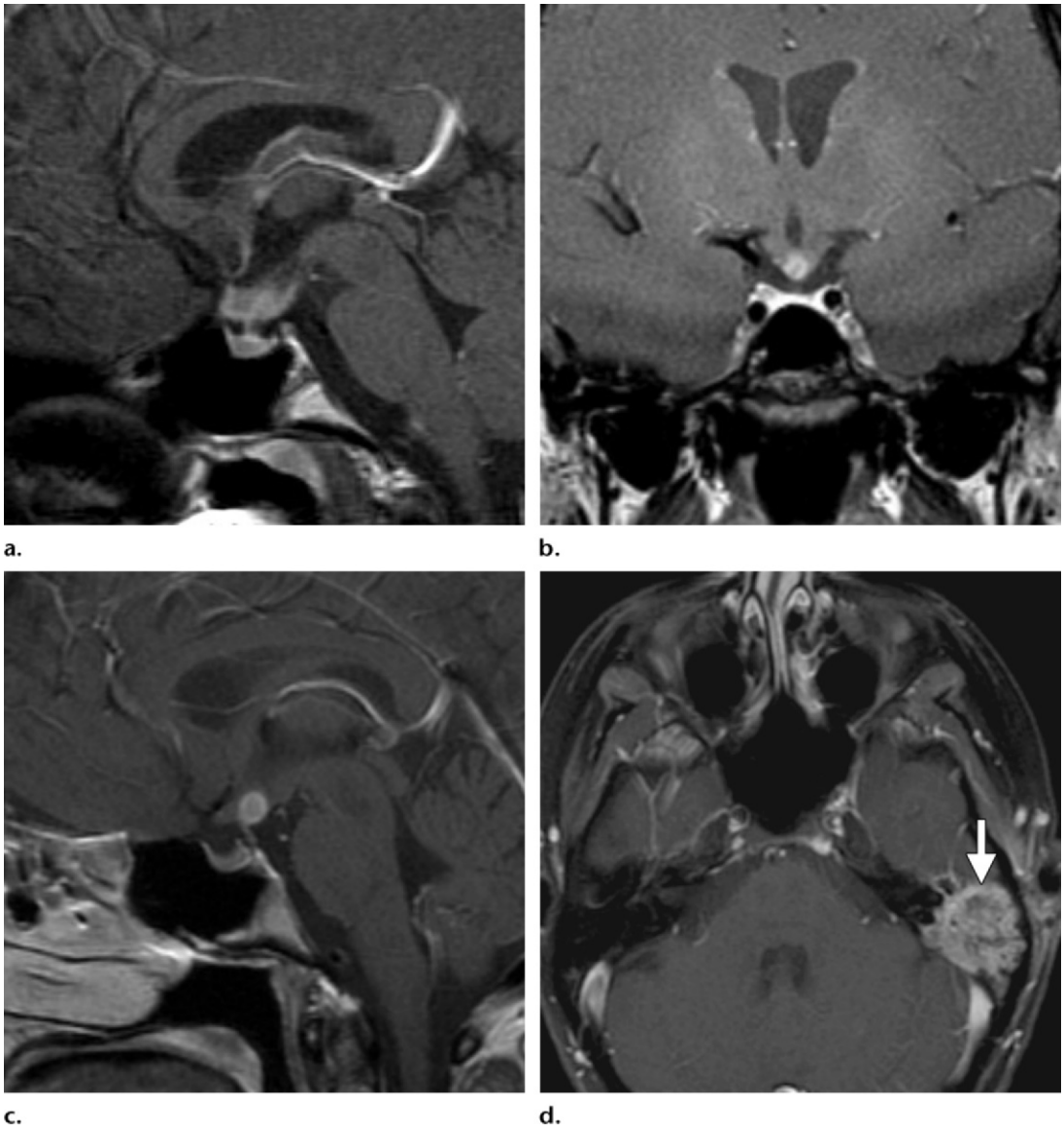

Figure 8. Anterior third ventricle masses in two pediatric patients. **(a, b)** Pilocytic astrocytoma in a 10-year-old patient. Sagittal **(a)** and coronal **(b)** contrast-enhanced T1-weighted MR images show solid, mildly enhancing infiltrative tissue involving the anterior contours of the third ventricle. At biopsy, the abnormality was determined to be a pilocytic astrocytoma (World Health Organization [WHO] classification grade I). **(c, d)** Langerhans cell histiocytosis in a 10-year-old patient. **(c)** Sagittal contrast-enhanced T1-weighted MR image shows focal nodular enhancement at the anterior aspect of the third ventricle. **(d)** Axial contrast-enhanced fat-saturated T1-weighted MR image shows a separate focus of abnormal irregular enhancement in the left temporal bone (arrow).

than at the posterior aspect of the ventricle, but in both cases it tends to have high attenuation at CT and intense solid enhancement at MR imaging. CSF spread should be carefully sought on gadolinium-enhanced MR images. In contrast, hypothalamic-chiasmatic pilocytic astrocytoma tends to have only mild enhancement and may be seen to extend locally along the optic tracts and nerves (18,19) (Fig 8). The heterogeneity of a craniopharyngioma and the presence of calcifications at CT are further clues to this diagnosis. Any of these lesions may manifest with diabetes insipidus, but craniopharyngioma is the only one that also commonly manifests with hypopituitarism (20).

In adult patients with anterior third ventricle masses, it is often difficult to differentiate these entities and the final diagnosis frequently depends on direct biopsy or CSF sampling (21,22).

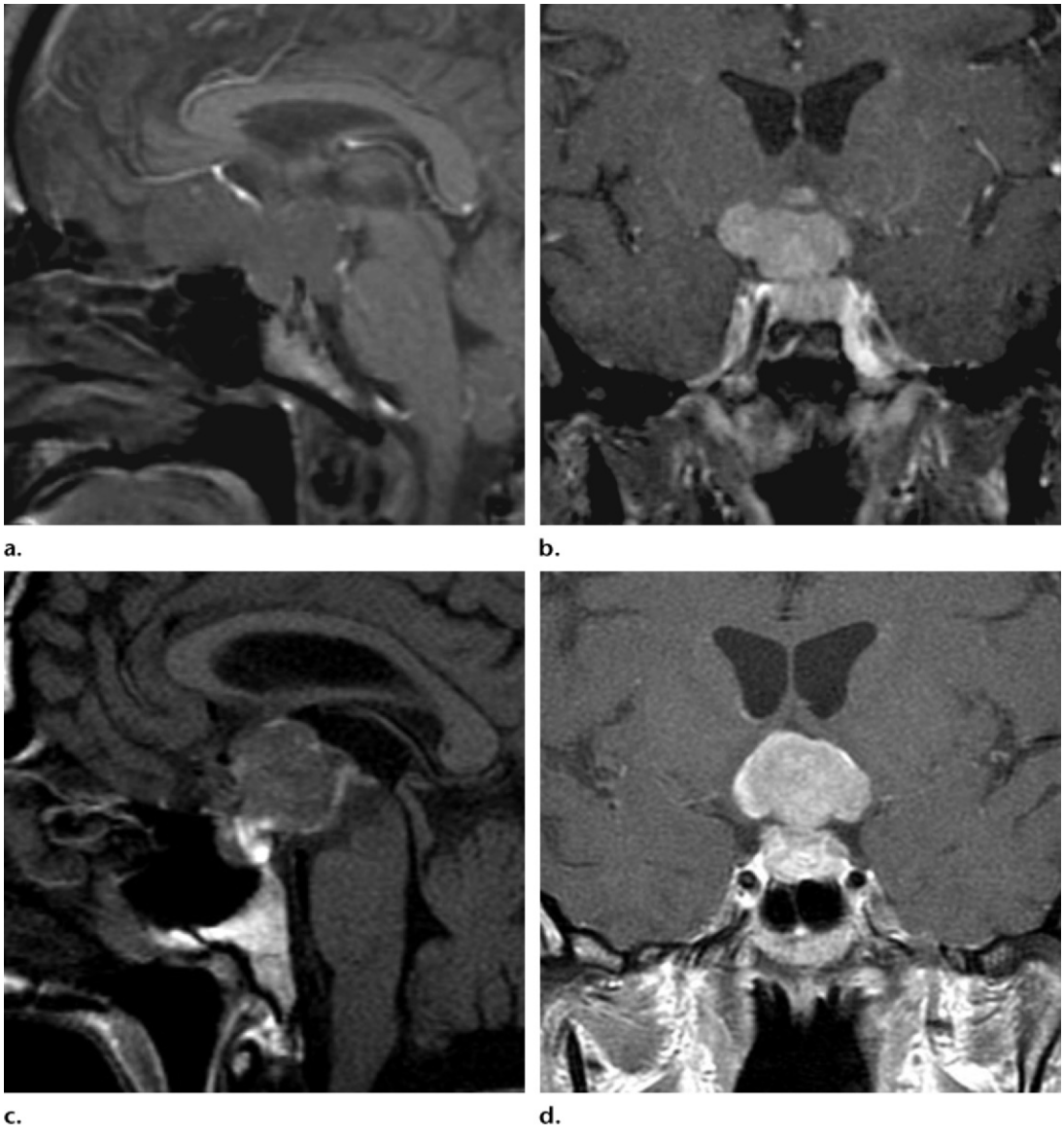

Figure 9. Similar-appearing anterior third ventricle masses in two adult patients. **(a, b)** Pituitary macroadenoma in a 68-year-old man with altered vision. Sagittal T1-weighted **(a)** and coronal contrast-enhanced T1-weighted **(b)** MR images show a lobulated sellar and suprasellar mass that distorts the anterior third ventricle. The mass has solid enhancement. At transsphenoidal surgery, it was determined to be a (nonsecretory) pituitary macroadenoma. **(c, d)** Metastatic disease in a 48-year-old man with diabetes insipidus and altered visual acuity. Sagittal T1-weighted **(c)** and coronal contrast-enhanced T1-weighted **(d)** MR images show a heterogeneous suprasellar mass that distorts the anterior third ventricle. Some intrinsic T1 hyperintensity is evident on the unenhanced image. The mass proved to be a metastasis from melanoma.

Pituitary macroadenoma is the most common of the adult pathologic processes affecting the anterior third ventricle and most often displaces rather than invades the ventricle (Fig 9). Papillary (adult-type) craniopharyngioma rarely has the calcifications seen in adamantinomatous (pediatric-type) craniopharyngioma and is more often a homogeneous solid mass (23,24). Lymphoma, metastases, and granulomatous disease may appear identical at CT and MR imaging. With any of these entities, it is important to look for evidence of CSF dissemination or additional brain or skull lesions that might allow narrowing of the differential diagnosis. Sellar meningiomas extending superiorly to deform the anterior third ventricle can be distinguished by means of their dural base and sclerosis of the adjacent skull base, if present.

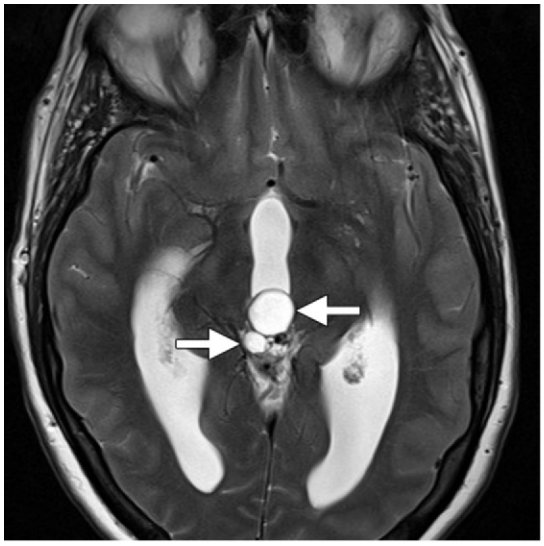

10a.

10b.

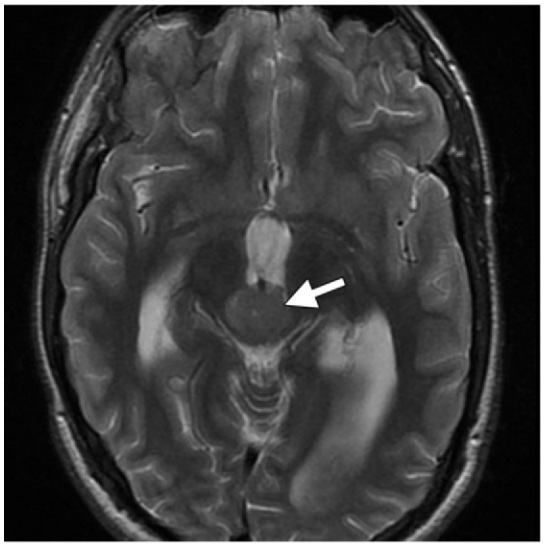

11a.

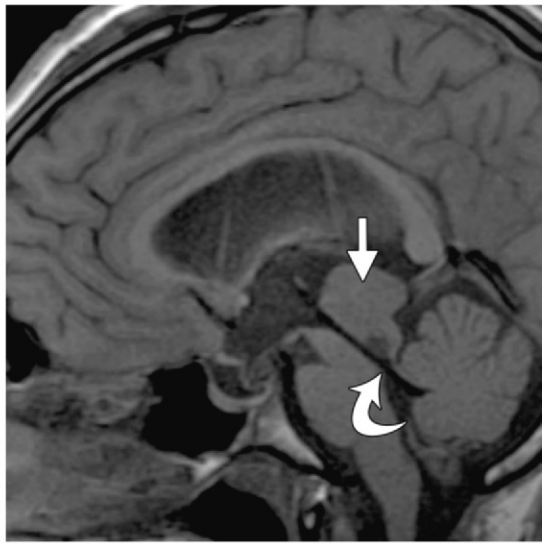

11b.

Figures 10, 11. **(10)** Pineocytoma in a 52-year-old woman with a 2-day history of worsening headaches and dizziness. **(a)** Axial T2-weighted MR image shows a multiloculated cystic mass (arrows) at the posterior aspect of the third ventricle. There is dilatation of the lateral and third ventricles. **(b)** Sagittal T1-weighted MR image shows that the complex cystic mass compresses the posterior commissure and obstructs the aqueduct (arrow). Minimal enhancement was seen on gadolinium-enhanced images. **(11)** Pineoblastoma in a 17-year-old boy with a 6-month history of headaches and intermittent diplopia. **(a)** Axial T2-weighted MR image shows a solid mass (arrow) at the posterior aspect of the obstructed third ventricle. **(b)** Sagittal T1-weighted MR image shows that the mass (straight arrow) is centered on the pineal gland with infiltration of the tectal plate. Gadolinium-enhanced images showed intense enhancement. A ventricular drain (curved arrow) was inserted through the aqueduct to relieve hydrocephalus.

Posterior Masses

The majority of posterior third ventricle masses are of pineal origin, with the most common neoplasm being a germinoma. However, results of pathologic analysis range from benign and typically asymptomatic cysts to pineocytomas (WHO grade II), pineoblastomas (WHO grade IV), other germ cell tumors, and teratomas (25,26). A recent article highlights the key imaging and clinical features that help distinguish these entities (25).

Most pediatric pineal tumors manifest as third ventricle obstruction and hydrocephalus when the tumor is still small (20). Pineal masses

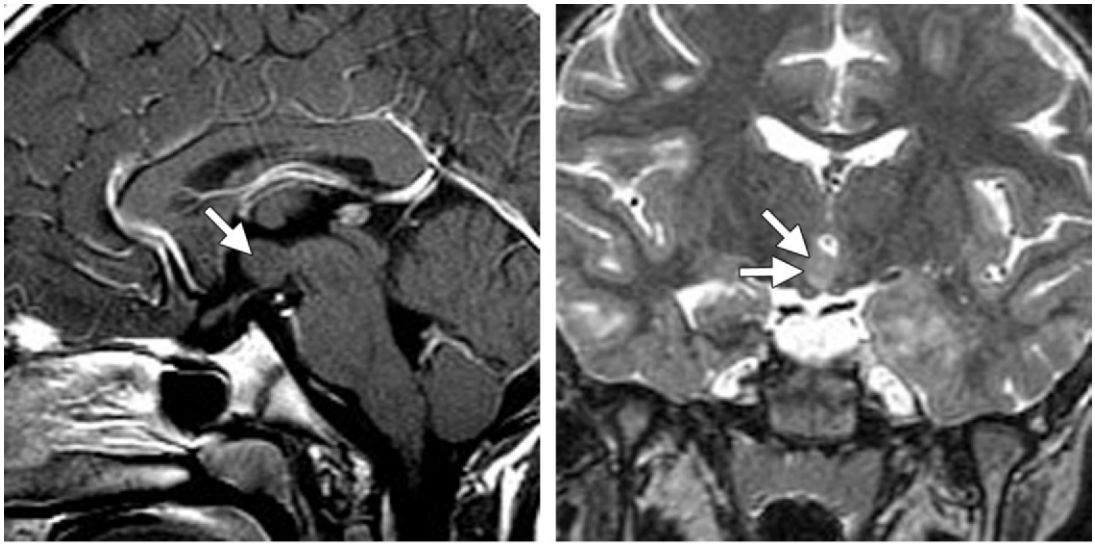

a. b.

Figure 12. Hypothalamic hamartoma in a 6-year-old girl with seizures. **(a)** Sagittal contrast-enhanced T1-weighted MR image shows a nonenhancing mass (arrow) in the floor of the third ventricle that is isointense relative to gray matter. **(b)** Coronal T2-weighted MR image shows that the mass (arrows) is subtly hyperintense relative to gray matter.

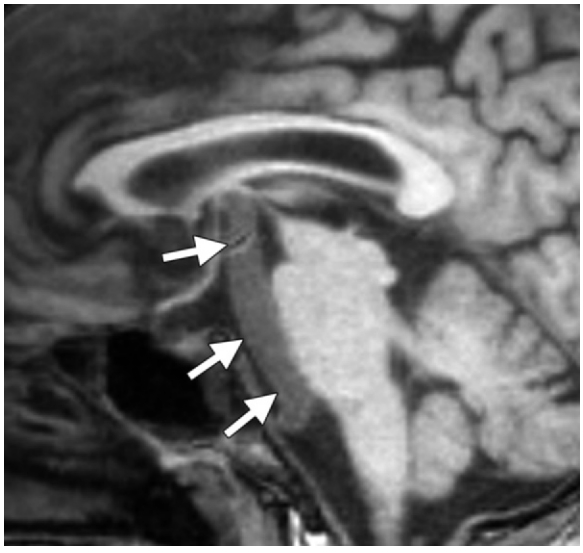

Figure 13. Dolichoectasia of the basilar artery in a 65-year-old man who was being evaluated for a neurodegenerative disorder. Sagittal T1-weighted MR image shows marked dolichoectasia of the basilar artery (arrows). As a result, the floor of the third ventricle is elevated to the level of the foramen of Monro.

in children or adults can also manifest as mass effect on the tectal plate, causing Parinaud syndrome (paralysis of upward gaze). Masses of the tectal plate itself, or less commonly of the inferior thalamus, may also distort the posterior third ventricle contour, resulting in aqueduct obstruction (Figs 10, 11).

Pineocytomas (WHO grade II) are slow-growing tumors composed of mature cells and most often occur in teens and young adults. They may mimic a cyst or appear aggressive, thus mimicking a pineoblastoma. Pineoblastomas (WHO grade IV) are highly malignant primitive tumors and typically arise in children or teens. The main differential diagnosis for these lesions is the more common germinoma, which has a significantly better prognosis.

Masses of the Ventricular Floor

Masses arising in the floor of the third ventricle are uncommon. The most frequently seen lesion is a hamartoma of the tuber cinereum (hypothalamic hamartoma). These nonneoplastic masses consist of heterotopic neurons and glia and typically manifest in childhood as central precocious puberty or gelastic seizures (27). At MR imaging, these lesions are isointense to gray matter on T1-weighted images and slightly hyperintense on T2-weighted images, with no enhancement on gadolinium-enhanced images (Fig 12). Extrinsic masses may also distort the floor of the third ventricle. Upward displacement of the floor can occur from ectasia of the basilar artery, a basilar artery aneurysm, or a dermoid, epidermoid, or arachnoid cyst of the prepontine cistern (Figs 13, 14).

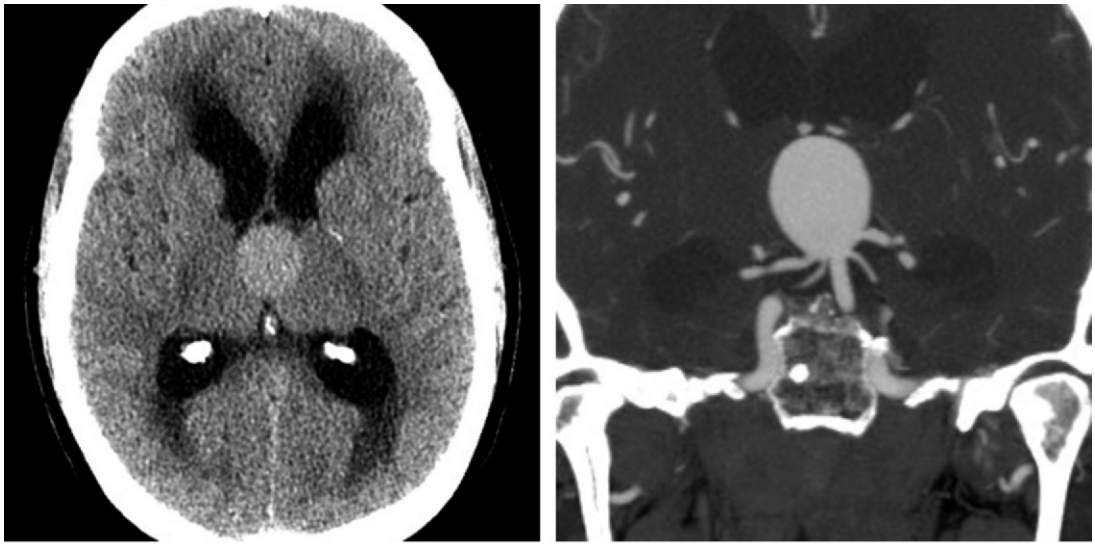

a. b.

Figure 14. Basilar artery aneurysm mimicking a colloid cyst in a 55-year-old woman. The patient had a preliminary diagnosis of colloid cyst and acute hydrocephalus. **(a)** Nonenhanced CT image shows a hyperattenuating mass at the foramen of Monro. **(b)** Coronal image from CT angiography shows that the mass is an aneurysm of the basilar artery tip.

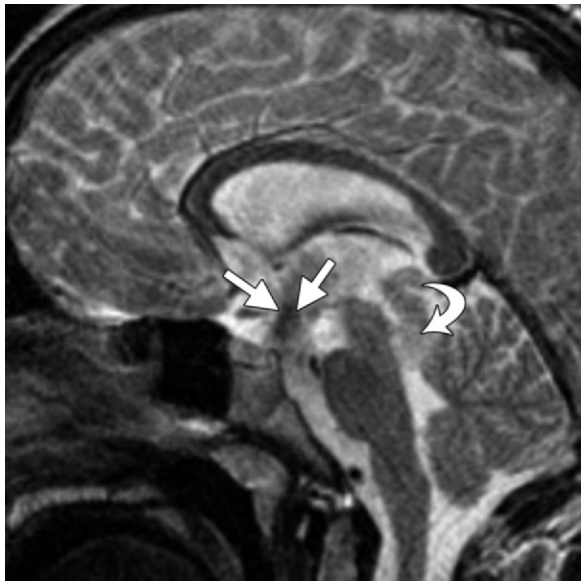

Figure 15. Defect from a third ventriculostomy in a 14-year-old boy. Sagittal T2-weighted MR image (3-mm section thickness) shows a tectal glioma (curved arrow), for which a third ventriculostomy was performed. Hypointense flow artifact (straight arrows) is seen due to CSF coursing through the ventriculostomy defect into the prepontine and suprasellar cisterns.

Third ventriculostomy involves creation of a perforation in the tuber cinereum to allow communication of the third ventricle with the prepontine cistern and is used to treat third ventricle obstruction. It is performed by means of a trajectory through one of the lateral ventricles and foramen of Monro, avoiding the fornix and caudate nucleus. An anomalous contour of the third ventricle floor (eg, the downward displacement that frequently occurs with long-standing hydrocephalus) should be noted at preoperative MR imaging to alert the surgeon before ventriculostomy (Fig 15) (28,29).

Teaching Point

Foramen of Monro Masses

Masses arising at the foramen of Monro frequently manifest as obstruction of the lateral ventricles. The most common true mass of the foramen of Monro is a colloid cyst, a benign lesion that

Figure 16. Colloid cyst. Sagittal T1-weighted MR image shows a heterogeneous cyst (straight arrow) at the foramen of Monro, posterior to the anterior commissure (arrowhead) and inferior to the fornix (curved arrow). There is dilatation of the lateral ventricles owing to obstruction of the foramen. Colloid cysts have many different appearances at CT and MR imaging. The anatomic location of a colloid cyst is one of the key aspects of making the diagnosis.

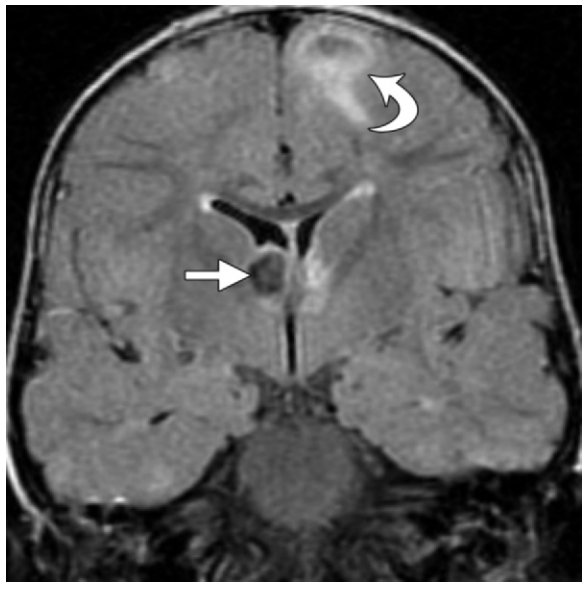

Figure 17. SGCT in a 9-year-old boy with known TSC. Coronal FLAIR image shows a large mass (straight arrow) at the foramen of Monro. The mass is hypointense due to calcification, which was evident at CT. A cortical tuber (curved arrow) is also evident in the left superior frontal gyrus.

occurs in adult patients (30). This well-defined round cyst may be from several millimeters to 3 cm in size and attaches to the anterior superior aspect of the third ventricle roof (Fig 16). Often hyperattenuating at nonenhanced CT, it has variable signal intensity at MR imaging and is often hyperintense on T1-weighted and FLAIR images. Peripheral gadolinium enhancement is rarely seen. Ninety percent of colloid cysts are asymptomatic and stable, while 10% are reported to enlarge or cause hydrocephalus. Rapid enlargement has been associated with coma and death (31).

The most common pediatric lesion of the foramen of Monro is an SGCT associated with TSC. It is found in up to 20% of patients with TSC and typically occurs in patients younger than 20 years (32). Subependymal nodules or hamartomas may occur anywhere along the ventricular surface in patients with TSC, but a nodule that enlarges over time and is greater than 1.3 cm raises concern about a neoplasm (33). SGCT is a low-grade astrocytoma (WHO grade I) that appears as a lobulated, heterogeneous, enhancing mass at the foramen of Monro and extends into the lateral or third ventricle. It may result in obstruction of the foramen. Cystic change, calcification, or hemorrhage may be present (Fig 17).

Subependymoma (WHO grade I) is a rare slow-growing tumor that most commonly occurs in the fourth ventricle in middle-aged to elderly patients. In the supratentorial brain, it favors the foramen of Monro and appears as a small (<2 cm), lobulated, well-defined lesion with minimal to moderate enhancement. It protrudes into the lateral ventricles more often than into the third ventricle (34,35). It may be an incidental finding or may obstruct the lateral ventricles (Fig 18). It is important to note that a key differential diagnostic point at MR imaging for all foramen of Monro lesions is CSF flow artifact.

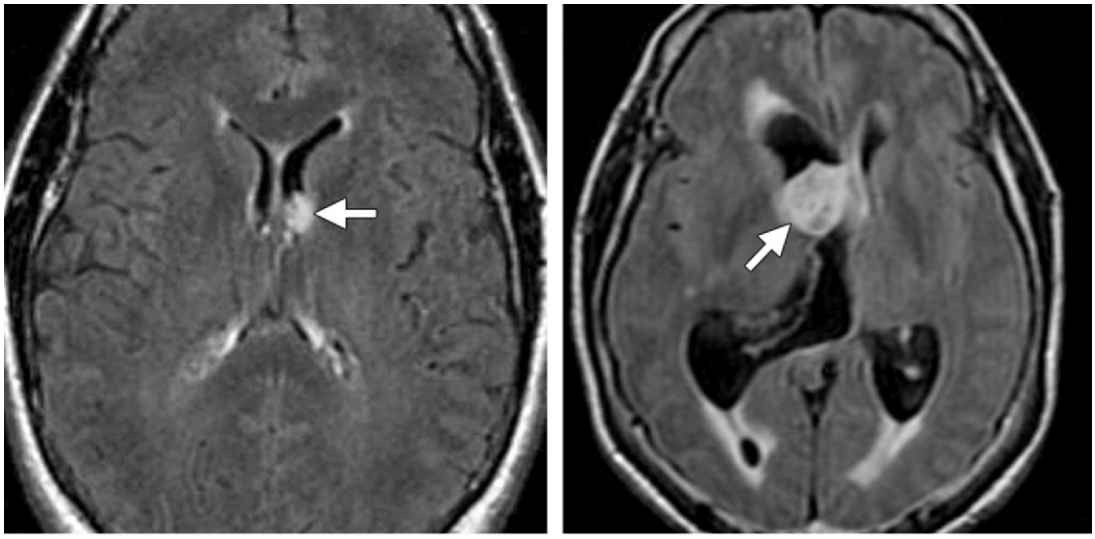

a. b.

Figure 18. Subependymoma of the foramen of Monro. **(a)** Subependymoma in an asymptomatic 69-year-old man. Axial FLAIR image shows a small well-defined nodule (arrow) at the foramen of Monro. There was no hydrocephalus. Minimal enhancement was seen on contrast-enhanced images. **(b)** Subependymoma in a 56-year-old man with a history of a foramen of Monro lesion who was acutely ill. Axial FLAIR image shows a larger more heterogeneous mass (arrow) that obstructs the foramen of Monro, causing dilatation of the lateral ventricles. The mass was partially calcified at CT.

Intraventricular Masses

Teaching Point

Purely intraventricular lesions of the third ventricle are rare. Intraventricular third ventricle masses are most often lesions of the choroid plexus (eg, primary choroid plexus papilloma [CPP] or choroid plexus carcinoma), a vascular malformation of the plexus, or a metastatic neoplastic or infectious lesion (eg, tuberculosis) seeding the plexus (36–38). Choroid plexus cysts are incidental benign neuroepithelial cysts in most patients but are of importance during fetal imaging. When they are found in association with other markers for chromosomal abnormality, amniocentesis should be considered (39). Primary lymphoma of the choroid plexus and secondary lymphoma seeding the plexus have been described. However, these entities are all relatively rare in the third ventricle, with choroid plexus masses being more common in the lateral ventricles and fourth ventricle.

Less commonly than choroid plexus lesions, intraventricular cysts (including congenital lesions and infectious entities such as neurocysticercosis) occur in the third ventricle. Rarely, purely intraventricular neoplasms such as meningioma, craniopharyngioma, and intraventricular glial neoplasms may be found (Table 1) (40–45).

CPP is a benign papillary neoplasm (WHO grade I) derived from choroid plexus epithelium. Up to 50% of CPPs occur in patients younger than 10 years; these lesions are most often found in the lateral ventricle. In adults, CPP is most often located in the fourth ventricle, but up to 5% of cases arise in the third ventricle (36,37) (Fig 19). CPP is associated with hydrocephalus due to CSF overproduction, mechanical obstruction, and impaired CSF resorption with hemorrhage. In the absence of clearly invasive features, it is difficult to distinguish CPP from choroid plexus carcinoma with imaging alone (38).

Chordoid glioma is a rare, slow-growing, noninvasive neoplasm (WHO grade II) containing both glial and chordoid histologic elements. It arises from the anterior third ventricle and is frequently adherent to the hypothalamus. At MR imaging, chordoid glioma appears as a well-defined ovoid mass that is isointense on T1-weighted images and enhances intensely with gadolinium (Fig 20). Cystic changes may be present, but calcification is rare (40). Complete resection appears to be curative, although it is often difficult to achieve due to the anatomic relationships of the tumor (41).

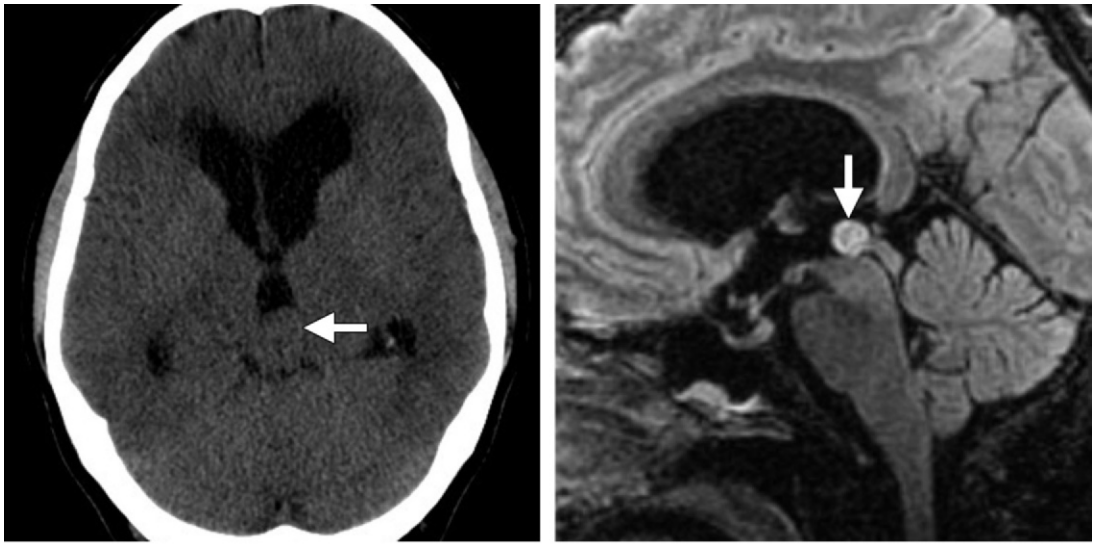

a. b.

Figure 19. CPP of the third ventricle in a 55-year-old man with a history of headaches for several months. **(a)** Axial nonenhanced CT image shows dilatation of the lateral ventricles and anterior third ventricle along with a subtle round mass (arrow), which is isoattenuating relative to the thalami. **(b)** Sagittal FLAIR image shows the small intraventricular mass (arrow) in the posterior third ventricle. The mass is separate from the pineal gland and appears to obstruct the aqueduct. Contrast-enhanced imaging showed solid enhancement. At surgery, the mass was found to be a CPP.

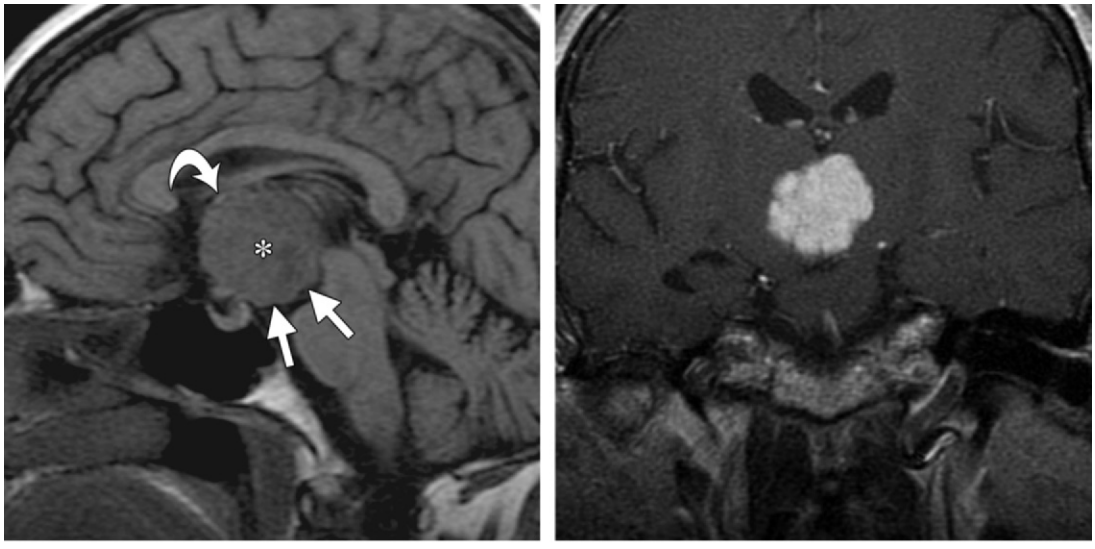

a. b.

Figure 20. Chordoid glioma in a 65-year-old woman with a 3-year history of cognitive decline, personality changes, and weight gain. **(a)** Sagittal T1-weighted MR image shows a round mass with lobulated margins (*) filling the anterior aspect of the third ventricle. The mass displaces the ventricular floor inferiorly (straight arrows) and elevates the anterior commissure (curved arrow). The mass was heterogeneous on T2-weighted images. **(b)** Coronal contrast-enhanced T1-weighted MR image shows diffuse intense enhancement of the mass.

Uncommonly, other neoplasms may arise entirely within the third ventricle, such as ependymoma, ganglioglioma, and glioblastoma multiforme (42–45). Metastatic seeding of the third ventricle by an intracranial neoplasm may also manifest as an intraventricular mass distinct from the choroid plexus (Fig 21) (46).

Summary

Most congenital malformations of the third ventricle are rare. The most common pediatric malformation is abnormal ventricular dilatation (hydrocephalus) due to aqueductal stenosis. A wide variety of pathologic processes may secondarily involve or arise in the third ventricle. To create a useful radiologic differential diagnosis, it is helpful to separate these lesions by their anatomic relationship to the ventricle while also considering the age of the patient.

The most commonly found pathologic processes are related to the anterior recesses of the third ventricle and are of sellar-suprasellar or hypothalamic-chiasmatic origin. Lesions deforming the posterior aspect of the third ventricle most commonly arise from the pineal gland, although tectal plate and inferior thalamic masses may obstruct the aqueduct, resulting in dilatation of the third ventricle. Lesions may arise in the floor of the third ventricle, such as hypothalamic hamartoma, or be extrinsic masses elevating the floor. The most common mass of the foramen of Monro is a benign colloid cyst. Most intraventricular masses are lesions arising in or metastatic to the choroid plexus.

MR imaging is recommended to best delineate the entire extent of a lesion involving the third ventricle and to further characterize it. To this end, sagittal MR imaging is often the most useful in determining from which direction a mass involves the third ventricle.

Teaching Point

RadioGraphics

***Disclosures of Potential Conflicts of Interest.*—A.G.O.:** *Related financial activities:* none. *Other financial activities:* board member for, royalties from, and stockholder in Amirsys and Amirsys Publishing; speaker for Covidien. **C.M.G.:** *Related financial activities:* none. *Other financial activities:* consultant for, royalties from, and stockholder in Amirsys. **K.L.S.:** *Related financial activities:* none. *Other financial activities:* consultant for, royalties from, and stockholder in Amirsys.

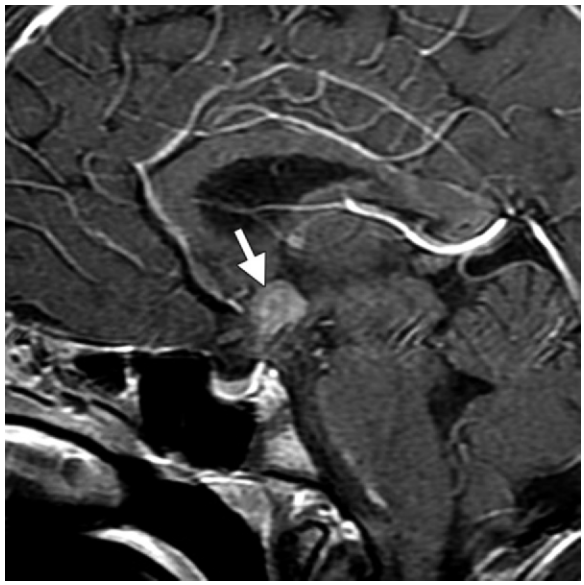

Figure 21. Metastatic intraventricular tumor in a 10-year-old girl with a history of a supratentorial parenchymal anaplastic ependymoma. The patient underwent resection of the tumor 2 years earlier followed by chemotherapy and radiation therapy. Sagittal contrast-enhanced T1-weighted MR image shows a large enhancing metastatic deposit (arrow) in the anterior recesses of the third ventricle. Small lateral ventricular nodules were also evident. Biopsy demonstrated intraventricular recurrence.

References

1. Harnsberger HR, Osborn AG, Macdonald AJ, Ross JS. Diagnostic and surgical imaging anatomy: brain, head and neck, spine. Salt Lake City, Utah: Amirsys, 2006; 49.
2. Standring S. Development of the nervous system. In: Standring S, Ellis H, Healy JC, Johnson D, Williams A, eds. Gray's anatomy. 39th ed. London, England: Churchill Livingstone, 2005; 260–267.
3. Standring S. Ventricular system and cerebrospinal fluid. In: Standring S, Ellis H, Healy JC, Johnson D, Williams A, eds. Gray's anatomy. 39th ed. London, England: Churchill Livingstone, 2005; 287–294.
4. Tubbs RS, Louis RG Jr, Wartmann CT, et al. The velum interpositum revisited and redefined. Surg Radiol Anat 2008;30(2):131–135.
5. Wen HT, Rhoton AL Jr, de Oliveira E. Transchoroidal approach to the third ventricle: an anatomic study of the choroidal fissure and its clinical application. Neurosurgery 1998;42(6):1205–1217; discussion 1217–1219.
6. Kier LE. The evolutionary and embryologic basis for the development and anatomy of the cavum veli interpositi. AJNR Am J Neuroradiol 2000;21(3): 612–614.
7. Wilder BG. The foramina of Monro: some questions of anatomical history. [Accessed online through http://www.NEJM.org/.] Boston Med Surg J 1880; 103:152–154.
8. Arvanitis LD, Sgantzos MN, Kotrotsios A, Vassiou KG. Congenital fusion of the thalami (atresia of the third ventricle) associated with parietooccipital meningocele. Pediatr Dev Pathol 2010;13(5):419–422.
9. Barkovich AJ. Hydrocephalus. In: Pediatric neuroimaging. 4th ed. Philadelphia, Pa: Lippincott Williams & Wilkins, 2005; 659–703.
10. Tisell M. How should primary aqueductal stenosis in adults be treated? A review. Acta Neurol Scand 2005;111(3):145–153.
11. Moore KR. Aqueductal stenosis. In: Osborn AG, Salzman KL, Barkovich AJ, eds. Diagnostic imaging: brain. 2nd ed. Philadelphia, Pa: Lippincott Williams & Wilkins, 2010; 20–23.
12. Steno A, Popp AJ, Wolfsberger S, Belan V, Steno J. Persisting embryonal infundibular recess. J Neurosurg 2009;110(2):359–362.

13. D'Addario V, Pinto V, Rossi AC, Pintucci A, Di Cagno L. Cavum veli interpositi cyst: prenatal diagnosis and postnatal outcome. Ultrasound Obstet Gynecol 2009;34(1):52–54.
14. Osborn AG. Ependymal cyst. In: Osborn AG, Salzman KL, Barkovich AJ, eds. Diagnostic imaging: brain. 2nd ed. Philadelphia, Pa: Lippincott Williams & Wilkins, 2010; 42–43.
15. Vlaho S, Gebhardt B, Gerlach R, Weidauer S, Kieslich M. Cyst of the third ventricle as an unusual cause of acquired hydrocephalus. Pediatr Neurol 2003;28(3):225–227.
16. Oppido PA, Fiorindi A, Benvenuti L, et al. Neuroendoscopic biopsy of ventricular tumors: a multicentric experience. Neurosurg Focus 2011;30(4):E2.
17. Steno J, Malácek M, Bízik I. Tumor-third ventricular relationships in supradiaphragmatic craniopharyngiomas: correlation of morphological, magnetic resonance imaging, and operative findings. Neurosurgery 2004;54(5):1051–1058; discussion 1058–1060.
18. Kollias SS, Barkovich AJ, Edwards MS. Magnetic resonance analysis of suprasellar tumors of childhood. Pediatr Neurosurg 1991-1992;17(6):284–303.
19. Liang L, Korogi Y, Sugahara T, et al. MRI of intracranial germ-cell tumours. Neuroradiology 2002;44 (5):382–388.
20. Barkovich AJ. Intracranial, orbital and neck masses of childhood. In: Pediatric neuroimaging. 4th ed. Philadelphia, Pa: Lippincott Williams & Wilkins, 2005; 506–658.
21. Johnsen DE, Woodruff WW, Allen IS, Cera PJ, Funkhouser GR, Coleman LL. MR imaging of the sellar and juxtasellar regions. RadioGraphics 1991; 11(5):727–758.
22. Choi SH, Kwon BJ, Na DG, Kim JH, Han MH, Chang KH. Pituitary adenoma, craniopharyngioma, and Rathke cleft cyst involving both intrasellar and suprasellar regions: differentiation using MRI. Clin Radiol 2007;62(5):453–462.
23. Miller DC. Pathology of craniopharyngiomas: clinical import of pathological findings. Pediatr Neurosurg 1994;21(suppl 1):11–17.
24. Behari S, Banerji D, Mishra A, et al. Intrinsic third ventricular craniopharyngiomas: report on six cases and a review of the literature. Surg Neurol 2003;60 (3):245–252; discussion 252–253.
25. Smith AB, Rushing EJ, Smirniotopoulos JG. Lesions of the pineal region: radiologic-pathologic correlation. RadioGraphics 2010;30(7):2001–2020.
26. Hirato J, Nakazato Y. Pathology of pineal region tumors. J Neurooncol 2001;54(3):239–249.
27. Saleem SN, Said AH, Lee DH. Lesions of the hypothalamus: MR imaging diagnostic features. RadioGraphics 2007;27(4):1087–1108.
28. Feng H, Huang G, Liao X, et al. Endoscopic third ventriculostomy in the management of obstructive hydrocephalus: an outcome analysis. J Neurosurg 2004;100(4):626–633.
29. Morota N, Watabe T, Inukai T, Hongo K, Nakagawa H. Anatomical variants in the floor of the third ventricle; implications for endoscopic third ventriculostomy. J Neurol Neurosurg Psychiatry 2000;69(4): 531–534.
30. Maeder PP, Holtås SL, Basibüyük LN, Salford LG, Tapper UA, Brun A. Colloid cysts of the third ventricle: correlation of MR and CT findings with histology and chemical analysis. AJNR Am J Neuroradiol 1990;11(3):575–581.
31. Osborn AG. Colloid cyst. In: Osborn AG, Salzman KL, Barkovich AJ, eds. Diagnostic imaging: brain. 2nd ed. Philadelphia, Pa: Lippincott Williams & Wilkins, 2010; 10–13.
32. Adriaensen ME, Schaefer-Prokop CM, Stijnen T, Duyndam DA, Zonnenberg BA, Prokop M. Prevalence of subependymal giant cell tumors in patients with tuberous sclerosis and a review of the literature. Eur J Neurol 2009;16(6):691–696.
33. Vezina G. Tuberous sclerosis complex. In: Osborn AG, Salzman KL, Barkovich AJ, eds. Diagnostic imaging: brain. 2nd ed. Philadelphia, Pa: Lippincott Williams & Wilkins, 2010; 98–101.
34. Im SH, Paek SH, Choi YL, et al. Clinicopathological study of seven cases of symptomatic supratentorial subependymoma. J Neurooncol 2003;61(1):57–67.
35. Salzman KL. Subependymoma. In: Osborn AG, Salzman KL, Barkovich AJ, eds. Diagnostic imaging: brain. 2nd ed. Philadelphia, Pa: Lippincott Williams & Wilkins, 2010; 68–71.
36. Koeller KK, Sandberg GD. Cerebral intraventricular neoplasms: radiologic-pathologic correlation. RadioGraphics 2002;22(6):1473–1505.
37. Nakano I, Kondo A, Iwasaki K. Choroid plexus papilloma in the posterior third ventricle: case report. Neurosurgery 1997;40(6):1279–1282.
38. Ho CY. Choroid plexus tumors. In: Osborn AG, Salzman KL, Barkovich AJ, eds. Diagnostic imaging: brain. 2nd ed. Philadelphia, Pa: Lippincott Williams & Wilkins, 2010; 72–81.
39. Osborn AG. Choroid plexus cyst. In: Osborn AG, Salzman KL, Barkovich AJ, eds. Diagnostic imaging: brain. 2nd ed. Philadelphia, Pa: Lippincott Williams & Wilkins, 2010; 38–41.
40. Rees JH. Chordoid glioma of the third ventricle. In: Osborn AG, Salzman KL, Barkovich AJ, eds. Diagnostic imaging: brain. 2nd ed. Philadelphia, Pa: Lippincott Williams & Wilkins, 2010; 56–57.
41. Vanhauwaert DJ, Clement F, Van Dorpe J, Deruytter MJ. Chordoid glioma of the third ventricle. Acta Neurochir (Wien) 2008;150(11):1183–1191.
42. Hauck EF, Vu L, Campbell GA, Nauta HJ. Intraventricular ganglioglioma. J Clin Neurosci 2008;15(11): 1291–1293.
43. Luther N, Souweidane MM. Neuroendoscopic resection of posterior third ventricular ependymoma: case report. Neurosurg Focus 2005;18(6A):E3.
44. Ragel BT, Townsend JJ, Arthur AS, Couldwell WT. Intraventricular tanycytic ependymoma: case report and review of the literature. J Neurooncol 2005;71 (2):189–193.
45. Lee TT, Manzano GR. Third ventricular glioblastoma multiforme: case report. Neurosurg Rev 1997; 20(4):291–294.
46. Shelton CH 3rd, Phillips CD, Laws ER, Larner JM. Third ventricular lesion masquerading as suprasellar disease. Surg Neurol 1999;51(2):177–180.

Masses and Malformations of the Third Ventricle: Normal Anatomic Relationships and Differential Diagnoses

Christine M. Glastonbury, MBBS • Anne G. Osborn, MD • Karen L. Salzman, MD

RadioGraphics 2011; 31:1889–1905 • **Published online** 10.1148/rg.317115083 • **Content Codes:** NR OI

Page 1892
Stenosis most often occurs in the proximal aqueduct and may be congenital or acquired as a postinflammatory aqueductal gliosis. Aqueductal stenosis and hydrocephalus may manifest at any time from fetal age to adulthood, with the age of presentation depending on the severity of the stenosis and hydrocephalus. Up to 10% of adult hydrocephalus cases are due to aqueductal stenosis (9–11).

Page 1895
When masses distort or invade the third ventricle, they most frequently arise in relation to the anterior aspect of the ventricle and can be broadly grouped into sellar-suprasellar masses and hypothalamic-chiasmatic masses.

Page 1900 (Figure on page 1900)
An anomalous contour of the third ventricle floor (eg, the downward displacement that frequently occurs with long-standing hydrocephalus) should be noted at preoperative MR imaging to alert the surgeon before ventriculostomy (Fig 15) (28,29).

Page 1902
Purely intraventricular lesions of the third ventricle are rare. Intraventricular third ventricle masses are most often lesions of the choroid plexus (eg, primary choroid plexus papilloma [CPP] or choroid plexus carcinoma), a vascular malformation of the plexus, or a metastatic neoplastic or infectious lesion (eg, tuberculosis) seeding the plexus (36–38).

Page 1904
A wide variety of pathologic processes may secondarily involve or arise in the third ventricle. To create a useful radiologic differential diagnosis, it is helpful to separate these lesions by their anatomic relationship to the ventricle while also considering the age of the patient.